

# Movement Artifacts in Helical CT Cone-Beam Reconstruction

Claas Bontus<sup>1</sup>, Roland Proksa<sup>1</sup>, Jan Timmer<sup>2</sup>, Thomas Köhler<sup>1</sup>, Michael Grass<sup>1</sup>

*Abstract*— We designed different dynamical CT phantoms and simulated a CT Cone-Beam scanner. The obtained projection data were used as input for three different reconstruction algorithms. Since the images show movement artifacts the comparison of different reconstruction algorithms for helical scanning yields information about the sensitivity of these algorithms to movement during the scanning procedure.

*Keywords*— CT reconstruction, Cone-Beam algorithms, Helical CT scanning, Movement artifacts.

## I. INTRODUCTION

THE next generation of medical CT scanners, viz. Cone-Beam scanners, necessitates sophisticated reconstruction algorithms. Those algorithms which are considered for practical purposes have to be evaluated for numerical stability, artifacts, reconstruction times and the sensitivity to all kinds of system imperfections. In a realistic environment movement is always involved during the scanning procedure. The patient and his/her organs never stay completely motionless. The evaluation of the different reconstruction algorithms with respect to motion artifacts is therefore another important aspect. We have designed different dynamical phantoms and tested the resulting level of artifacts for different helical reconstruction algorithms. In particular we restricted ourselves to the evaluation of approximative algorithms, which are of the back-projection type. For the comparison with a well known acquisition scheme we used single detector row circular reconstruction (filtered back-projection) as a gold standard.

## II. SCANNER GEOMETRY

For the simulations we used a CT scanner with 40 detector lines and 1024 elements per line. We set the detector height equal to 35.34 mm and its width to 904.7 mm, which corresponds to a fan-angle of 56.96 degrees. The distance of the focal spot to the rotation axis was chosen to be 515 mm and the distance of the focal spot to the detector center was equal to 910 mm. The scanner's rotation time was set to 0.5 s (2 Hz).

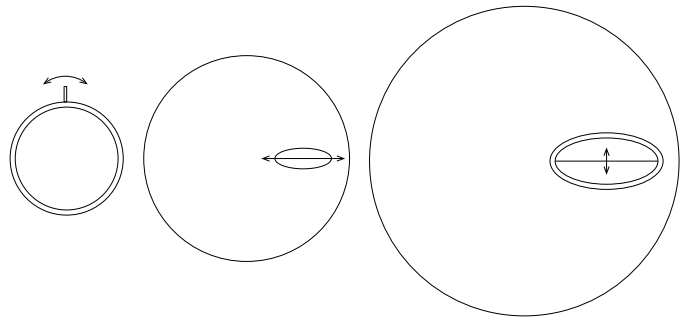
For helical scanning we performed simulations with two different acquisition schemes, viz. 1-PI and 3-PI mode. In the 1-PI mode the pitch was set equal to 32.64 mm per rotation for the head-phantom (see below) and to 26.04 mm for the abdomen phantoms. In the 3-PI mode it was set equal to 11.97 mm per rotation for the head-phantom and to 10.34 mm for the abdomen phantoms.

<sup>1</sup> Philips Research Laboratories, Division Technical Systems, Röntgenstraße 24-26, 22335 Hamburg, Germany

<sup>2</sup> Philips Medical Systems, Veenpluis 4-6, 5680 DA Best, The Netherlands

## III. PHANTOM DESIGN

In the following subsections we describe the phantoms in detail. They are composed of mathematical objects with different densities. Some of these objects oscillate during the scanning procedure. For our analysis we have chosen relatively high frequencies and amplitudes compared to a realistic case. By this way we realized a scenario that covers the worst possible case. The following images indicate the location of the mathematical objects within the phantoms. The arrows illustrate the movement.



### A. Head phantom

This phantom is intended to approximate movement of the septum, which can result in severe artifacts in clinical scanning. The phantom is composed of a cylinder with a radius of 80 mm consisting of water. The cylinder is surrounded by a shell with a thickness of 10 mm consisting of bone. The symmetry axis of the cylinder coincides with the scanner's rotation axis. Moreover, a box with a thickness of 2 mm and a length of 22.5 mm is connected to the outer shell. This box also consists of bone and is supposed to approximate the septum. For the simulation of the movement we let this box oscillate with an amplitude of five degrees and a frequency of 1.51 Hz.

### B. Abdomen phantom, colon movement

During inspections of the abdomen colon movement can also result in artifacts. We therefore designed a phantom, which is composed of a cylinder consisting of water. This cylinder has a radius of 170 mm and its symmetry axis coincides with the rotation axis. For the simulation of the colon we placed an ellipsoid consisting of air inside the cylinder. It has a horizontal radius of 50 mm, a vertical radius of 20 mm and was placed such that its center is located on the horizontal axis 90 mm from the center of rotation. For the movement simulation we let this ellipsoid

oscillate horizontally with an amplitude of 10 mm and a frequency of 2.23 Hz.

### C. Abdomen phantom, bladder movement

In a third simulation we studied changes of the water level in the bladder. For this we approximated the abdomen by a cylinder with radius 240 mm consisting of water. The bladder was approximated by an ellipsoid with horizontal radius 90 mm, vertical radius 30 mm and longitudinal radius 30 mm. It was placed on the horizontal axis with its center located 130 mm from the center of rotation. The bladder is surrounded by an outer shell consisting of muscle with a thickness of 10 mm. Its interior consists of water in the lower half and of air in the upper one. For the simulation of the movement we made the water level oscillate vertically with an amplitude of 5 mm and a frequency of 1.75 Hz.

## IV. RECONSTRUCTION ALGORITHMS

For our analysis we compared the results of three different helical reconstruction algorithms with classical circular reconstruction. In the following we give a short summary of the reconstruction algorithms used. Each algorithm is an approximative algorithm and of the filtered back-projection (FBP) type.

### A. The PI-Method

The PI-Method [1] is based on the so-called PI-sufficiency condition, which requires that each object point gets illuminated over an angular range of 180 degrees. The pitch mentioned above is chosen such that the acquisition fulfills this requirement.

For the reconstruction the first step, which has to be performed, is a parallel rebinning row by row. This yields data on a virtual planar detector containing the rotation axis. In the next steps the rebinned data are weighted, filtered row wise and back-projected.

### B. The Three-PI-Method

The  $n$ -PI-Methods [2] are a generalization of the PI-Method. They provide the possibility to choose a smaller pitch and to use the resulting redundant data. In particular the algorithm necessitates that each voxel gets illuminated over an angular range of  $n \times 180$  degrees. For the study presented here we have restricted ourselves to the case  $n = 3$ , i.e. the 3-PI-Method.

Rebinning is again the first step of the reconstruction algorithm. It yields data on a virtual rectangular detector containing the rotation axis. Weighting and ramp filtering of the data have to be performed before the back-projection step results in the reconstructed images.

### C. Advanced single slice rebinning

Advanced single slice rebinning (ASSR) [3] is a reconstruction algorithm for which tilted planes are reconstructed using classical two-dimensional filtered back-projection. The system pitch can be chosen equal to the value of the PI-Method.

In particular the algorithm requires the projection data to be rebinned onto tilted virtual planes. These data have to be weighted with factors taking the tilt angle and a length correction into account. Finally 2D filtered back-projection yields image data on slices which are not orthogonal to the rotation axis. The longitudinal distance between these slices is chosen smaller than the obtainable resolution. Using an interpolation step a certain number of these planes are averaged in order to improve the image quality.

## V. RESULTS AND DISCUSSION

Movement during the scanning procedure results in artifacts in the reconstructed images. A closer look onto the details can yield valuable information about the origin of the artifacts. In the following we summarize our observations.

Figs. 1–4 contain reconstruction results of the head phantom. The two images within each figure show the best and worst obtained results for each reconstruction method under consideration. Fig. 1 shows the artifacts which result from the same phantom in classical circular scanning in combination with a single-line scanner and filtered back-projection.

Figs. 5–8 contain reconstruction results of the first abdomen phantom. We restrict ourselves to images showing the worst obtained artifacts for each reconstruction method.

Comparing the images we draw the following conclusions:

1. The 3-PI-Method yields the best images. Circular filtered back-projection proves to perform better than ASSR and 1-PI. The latter two yield images of comparable quality. In order to put these observations on a more stable ground we computed the root-mean-squared (RMS) of the hounsfield values in the central parts, i.e. the water cylinder, in Figs. 1–4. The corresponding numbers for those slices which contain the worst artifacts are 3.82, 6.84, 10.3 and 12.8 for 3-PI, circular, ASSR and 1-PI, resp.
2. For each considered reconstruction algorithm we can define a relation between the first projection which contributes to one particular reconstruction plane and the position of the moving object. As it turns out the severity of the artifacts strongly depends on this position. This holds true for each algorithm considered.
3. Movement artifacts can have different shapes. In the best case they are hardly visible at all. In the worst case they can result in the non-visibility of small details or in curved streaks in the reconstructed images.
4. As mentioned above the phantoms are exaggerated concerning the movements' frequencies and amplitudes. As an additional result we observed that smaller frequencies and/or amplitudes tend to decrease the movement artifacts only slightly.

In order to understand why the artifacts are differently distinct we have to remember the algorithms' details. For ASSR and the 1-PI-Method projection data taken over an angular range of 180 degrees are back-projected. For circu-

lar filtered back-projection the angular range corresponds to 360 degrees and for the 3-PI-Method it corresponds to 540 degrees. We therefore conclude that a larger angular range provides the possibility that inconsistencies due to movement get averaged out.

In summary we observe that the shape of the artifacts varies significantly with the used reconstruction algorithms and the strength of the artifacts depends also on the method used. Before the decision if a particular algorithm is suitable for clinical scanning can be taken, the comparison with well-known protocols is necessary. For this study we used circular scanning as gold standard. The considered helical algorithms result in artifacts which are comparable to those of this gold standard. While the 3-PI-Method seems to be even less sensitive to movement, ASSR and the 1-PI-Method yield only slightly worse images than circular filtered back-projection.

#### REFERENCES

- [1] P.E. Danielsson, P. Edholm, J. Eriksson, M. Magnusson-Seger, "Towards exact 3D-reconstruction for helical cone-beam scanning of long objects", *Proceedings of the 3D'97 conference*, Nemacon, Pennsylvania, USA 1997, pp. 141-144.
- [2] R. Proksa, Th. Köhler, M. Grass, J. Timmer, *IEEE Transactions on medical imaging*, Vol. 19, No. 9, pp. 848-863, 2000.
- [3] M. Kachelrieß, S. Schaller, W.A. Kalender, *Medical Physics*, Vol. 27, No. 4, pp. 754-772, 2000.

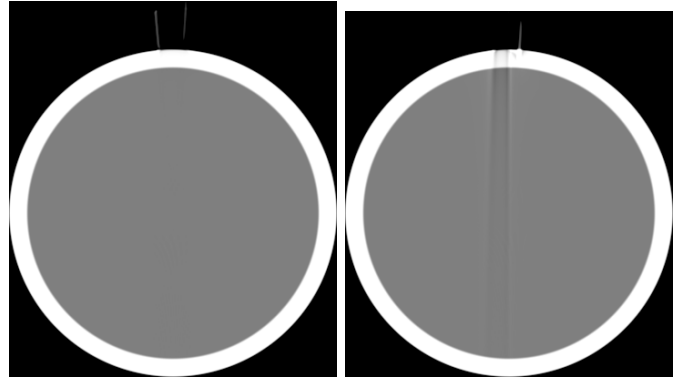


Fig. 1. The head phantom scanned in single-slice circular mode. Level: 0 HU, Window: 1000 HU.

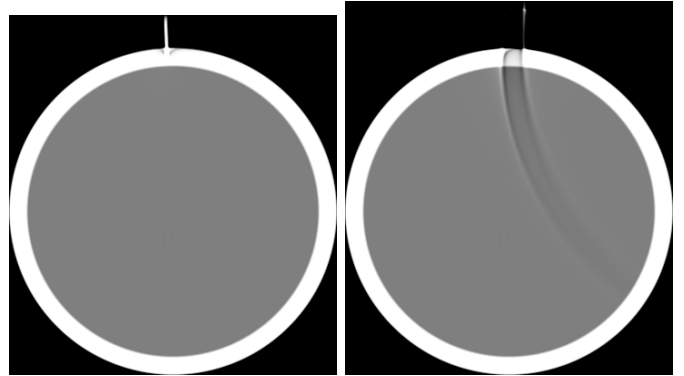


Fig. 2. Head phantom: 1-PI-Method.

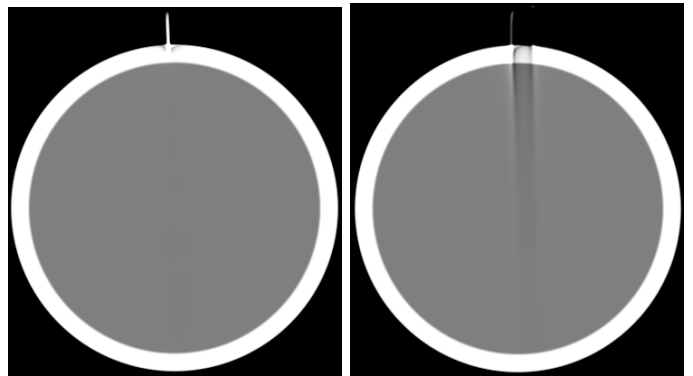


Fig. 3. Same as Fig. 2 but for the ASSR method.

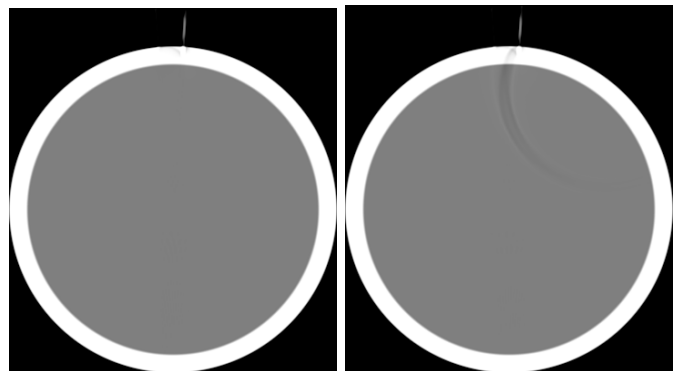


Fig. 4. Same as Fig. 2 but for the 3-PI-Method.

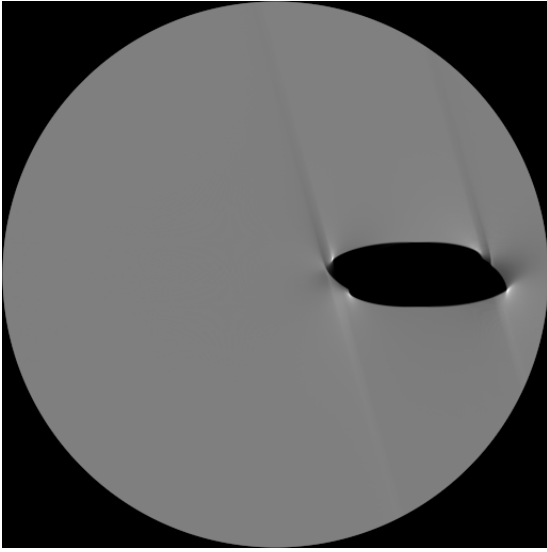


Fig. 5. Simulation of colon movement. Circular scanning, Level: 0 HU, Window: 1000 HU.

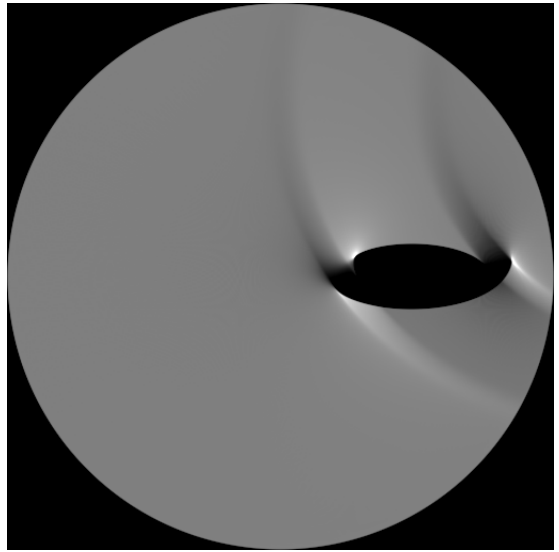


Fig. 7. Same as Fig. 5 but for the ASSR Method.

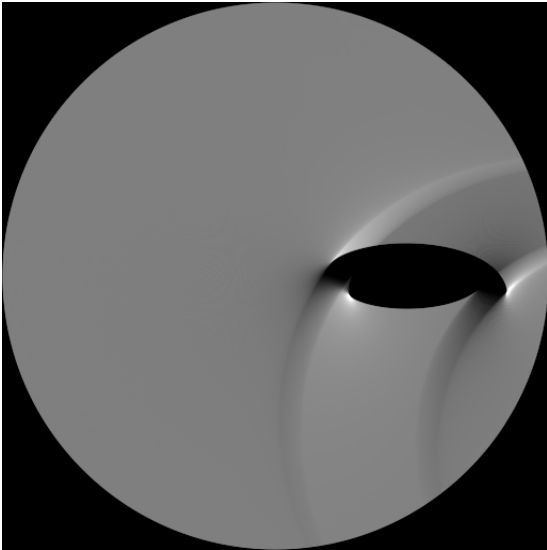


Fig. 6. Same as Fig. 5 but for the 1-PI-Method.

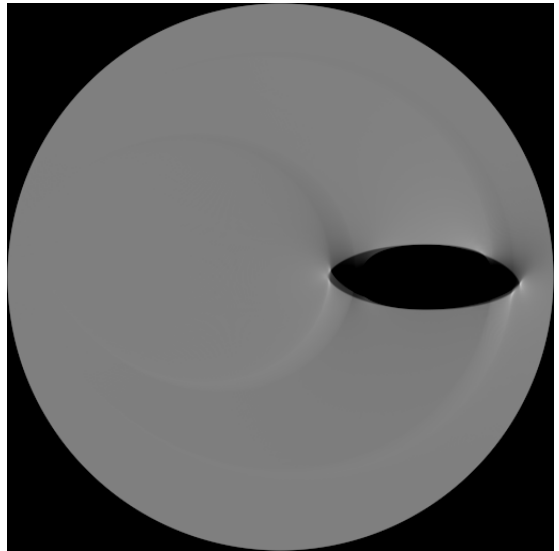


Fig. 8. Same as Fig. 5 but for the 3-PI-Method.